

# Spectral Puzzle of the Off-Axis Gamma-Ray Burst in GW170817

Kunihito Ioka<sup>1</sup><sup>★</sup> and Takashi Nakamura,<sup>2</sup>

<sup>1</sup>*Center for Gravitational Physics, Yukawa Institute for Theoretical Physics, Kyoto University, Kyoto 606-8502, Japan*

<sup>2</sup>*Department of Physics, Kyoto University, Kyoto 606-8502, Japan*

Accepted XXX. Received YYY; in original form ZZZ

## ABSTRACT

Gravitational waves from a merger of two neutron stars (NSs) were discovered for the first time in GW170817, together with diverse electromagnetic counterparts, providing a direct clue to the origin of short gamma-ray bursts (sGRBs). The associated sGRB 170817A was much fainter than typical, suggesting off-axis emission from a relativistic jet. However the observed prompt spectrum is inconsistent with the spectral (Amati) relation and causes the compactness problem in the simplest off-axis model. We focus on this spectral puzzle and suggest a possible key that the off-axis emission generally comes from the off-center jet, neither the jet core nor the line-of-sight jet, if the jet structure is exponentially faint outward as inferred from observations. The off-center jet could be loaded with baryon or cocoon. The off-axis model predicts that roughly  $\sim 10\%$  events are brighter at smaller viewing angles than sGRB 170817A, although the exact event rate sensitively depends on uncertainties of the off-center structure. The model also predicts outliers to Amati relation, providing future tests to reveal the central engine activities.

**Key words:** gravitational waves – radiation mechanisms: general – relativistic processes – stars: jets – gamma-ray burst: individual: GRB 170817A – gamma-rays: general

## 1 INTRODUCTION

What is the origin of short gamma-ray bursts? This is a long-standing problem for more than 40 years (e.g., [Nakar 2007](#); [Berger 2014](#)). A merger of binary neutron stars has been thought to be the most promising candidate (e.g., [Paczynski 1986](#); [Goodman 1986](#); [Eichler et al. 1989](#)), although an unequivocal evidence was missing. The detection of the gravitational wave (GW) event GW170817 ([Abbott et al. 2017a](#)) and the associated electromagnetic counterparts ([Abbott et al. 2017b](#)) revolutionized the situation. In particular, the short gamma-ray burst sGRB 170817A detected two seconds ( $\sim 1.7$  s) after GW170817 ([Abbott et al. 2017c](#); [Goldstein et al. 2017](#); [Savchenko et al. 2017](#)) and the following afterglows in radio to X-ray ([Troja et al. 2017](#); [Margutti et al. 2017](#); [Haggard et al. 2017](#); [Hallinan et al. 2017](#); [Alexander et al. 2017](#); [Lyman et al. 2018](#)) give the first direct clues to this problem.

The problem has not been solved yet because sGRB 170817A was very weak with an isotropic-equivalent energy  $E_{\gamma, \text{iso}} \sim 5.35 \times 10^{46}$  erg, which is many orders of magnitude

smaller than ordinary values. On the other hand, the afterglow observations, in particular of superluminal motion in radio ([Mooley et al. 2018b](#); [Ghirlanda et al. 2018](#)) and the consistency between the spectral index and the light curve slope after the luminosity peak ([Troja et al. 2018b](#); [Mooley et al. 2018c](#); [Lamb et al. 2019](#)), strongly suggest that a relativistic jet is launched and successfully breaks out the merger ejecta in this event ([Nagakura et al. 2014](#); [Murguia-Berthier et al. 2014](#)).

[Ioka & Nakamura \(2018\)](#) proposed that sGRB 170817A is faint because the jet is off-axis to our line-of-sight (see also [Abbott et al. 2017c](#); [Granot et al. 2017, 2018](#); [Lamb & Kobayashi 2018](#)). Most emission is beamed into the on-axis direction via a relativistic effect and an off-axis observer receives photons emitted outside the beaming cone. Consequently the apparent energy of the off-axis jet becomes faint ([Ioka & Nakamura 2001](#); [Yamazaki et al. 2002, 2018](#)). The off-axis model is initially studied by using a top-hat jet with uniform brightness and a sharp edge. This zeroth-order approximation is useful to capture the essential features of the off-axis model. Taking the effect of a finite opening angle of the jet, a typical jet with a typical viewing angle is found to be broadly consistent with the observations.

<sup>★</sup> E-mail: kunihito.ioka@yukawa.kyoto-u.ac.jp (KI)

However the simplest off-axis model seems to be difficult to explain the spectral peak energy  $\nu_{\text{peak}} = 185 \pm 62$  keV of the main pulse of GRB 170817A, if the central value is adopted. The de-beamed emission from an off-axis top-hat jet tends to have a low peak energy  $\nu_{\text{peak}} \sim 10$  keV, or the peak energy viewed on-axis is required to be very high  $> 10$  MeV (Kasliwal et al. 2017; Ioka & Nakamura 2018; Matsumoto et al. 2019). More precisely, if the jet is viewed on-axis, the isotropic energy and the peak energy do not satisfy the well-known relation, so-called Amati relation for sGRBs (Amati et al. 2002; Yonetoku et al. 2004; Tsutsui et al. 2013), which is  $\sim 100$  times dimmer than that for long GRBs at the same peak energy  $\nu_{\text{peak}}$ . Furthermore the afterglow observations including VLBI observations of superluminal motion reveal a jet with energy  $E_{\text{iso}} > 10^{52}$  erg, a narrow core  $\theta_c \lesssim 5^\circ$  and a viewing angle  $\sim 14^\circ - 28^\circ$  (Mooley et al. 2018b; Ghirlanda et al. 2018). If we adopt these parameters for an off-axis top-hat jet, the compactness problem is serious (Matsumoto et al. 2019).<sup>1</sup> In the previous paper, we put the above spectral puzzle aside partly because the error bar is large and the puzzle is solved if we allow  $3\sigma$  error (Ioka & Nakamura 2018). However the large error bar could mainly stem from the spectral evolution during the burst and the peak energy of the main pulse could be really high (Veres et al. 2018). The another reason for neglecting the spectral puzzle is that the weak tail with 34% of the fluence of the main pulse has a temperature  $k_B T = 10.3 \pm 1.5$  keV, consistent with the simplest off-axis model. The main pulse could be produced by a different mechanism, such as scattering of an sGRB by a cocoon (Kisaka et al. 2015, 2017, 2018) and a cocoon breakout from ejecta (Kasliwal et al. 2017; Gottlieb et al. 2018; Nakar et al. 2018; Ioka et al. 2019).

The approximation of a top-hat jet would be too simple to discuss the spectral puzzle (Mészáros et al. 1998; Zhang & Mészáros 2002). The afterglow observation, in particular the slowly-rising light curve, is not consistent with a top-hat jet (Mooley et al. 2018a), but strongly suggests a structured jet (Troja et al. 2018a; Ruan et al. 2018; Margutti et al. 2018; D’Avanzo et al. 2018; Lazzati et al. 2018; Lyman et al. 2018; Troja et al. 2018b; Ghirlanda et al. 2018; Lamb et al. 2019). The jet structure most likely affects the prompt emission and its spectrum as well.

In this paper we reexamine the spectrum of an off-axis jet in GW170817 taking the jet structure constrained by the afterglow observations into account. We suggest a possible solution, in which the off-axis emission from a typical sGRB jet is compatible with sGRB 170817A. In Sec. 2, we summarize the jet structure inferred from the afterglow observations. In Sec. 3, we generalize the formulation in Ioka & Nakamura (2001) to calculate the off-axis emission from a structured jet. In Sec. 4, we show that the off-axis emission mostly comes from the off-center jet, neither the jet core nor the line-of-sight jet, if the jet structure is exponentially faint outward, and the off-center emission can solve the spectral puzzle. Section 5 is devoted to summary and discussions.

<sup>1</sup> The compactness problem is in principle avoidable if the spectral cutoff above the peak energy is extremely sharp, which is not known from the observations of sGRB 170817A (Ioka & Nakamura 2018).

## 2 JET STRUCTURE FROM AFTERGLOW OBSERVATIONS

Before discussing the off-axis emission, we summarize the jet structure inferred from the observations of the afterglows in Fig. 1. The solid and dashed lines show the gamma-ray energy of each model specified by different color as a function of an angle  $\theta$  from the jet center. The afterglow of sGRB 170817A was observed after  $\sim 10$  days from the prompt sGRB, and the solid line part of the jet emission was not observed at  $\sim 10$  days since only the part with  $\theta > \theta_v - \Gamma^{-1}$  has a significant contribution to the afterglow radiation, where  $\Gamma$  and  $\theta_v$  are the Lorentz factor of the emitting region and the viewing angle, respectively. Here we obtain  $\Gamma$  assuming that each fluid element at each angle follows the spherical hydrodynamical evolution decelerated in the interstellar medium because numerical simulations suggest that this is a good approximation (Kumar & Granot 2003; van Eerten et al. 2010). Note that the Lorentz factor  $\Gamma$  in the afterglow phase is basically different from that in the prompt phase.

As time goes, the angular size  $\Gamma^{-1}$  expands. Then we can progressively probe the jet structure outside the angular size observable at  $\sim 10$  days, in particular the inner part close to the jet axis because the inner jet dominates the energy and the flux. However we can not infer the structure of the dashed region because the emission from this region is integrated in the initial observation at  $\sim 10$  days. Thus the dashed lines are the part unconstrained by the afterglow observations. The observations of the afterglow start at  $\sim 10$  days and there is no information before that. At this time,  $\sim 10$  days, we are already observing an angular size of  $\sim 1/\Gamma$  around the line-of-sight in the jet.

In Fig. 1, we assume a radiative efficiency  $\epsilon_\gamma = 10\%$ , which is typical for the observed sGRBs (e.g., Fong et al. 2015). These structures are obtained by assuming a functional form of the jet structure, calculating the afterglow emission with the standard afterglow theory, and fitting the afterglow observations with model parameters such as the ambient density  $n$ , the viewing angle of the jet  $\theta_v$ , the total energy, and so on. The different structures obtained by different authors most likely reflect the difference of the assumed structure and model parameters, which are not completely determined only by the light curve observations.

In Fig. 1, we also plot the isotropic energy of sGRB 170817A at the viewing angle of the jet (*cross marks*) to compare it with the jet structure. Note that the VLBI observations of superluminal motion prefer a viewing angle of  $14^\circ \lesssim \theta_v \lesssim 28^\circ$  (Mooley et al. 2018b). Note also that in blue, cyan and purple line cases, the gamma-ray energy exceeds that of sGRB 170817A, requiring smaller radiative efficiency than  $\epsilon_\gamma = 10\%$  at the viewing angle.

From Fig. 1, we can find that the central part should be much more energetic than the observed sGRB 170817A, regardless of the different structures obtained by the different authors. In order not to exceed sGRB 170817A, the isotropic gamma-ray energy of the jet should decrease exponentially outward (where it is not always Gaussian but a sharply decreasing function). This is a general property required from the afterglow and sGRB 170817A. Therefore we adopt a fiducial case as

$$E_\gamma(\theta) = \epsilon_\gamma E_0 \exp(-\theta^2/2\theta_c^2), \quad (1)$$

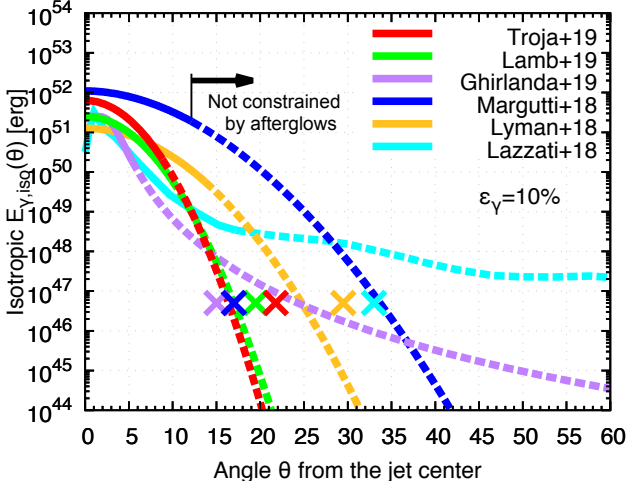


**Figure 1.** The jet structures inferred from the observations of the afterglow light curves (solid lines) are plotted, where a radiative efficiency  $\epsilon_\gamma = 10\%$  is assumed. The dashed lines show the part unconstrained by the afterglow observations. The isotropic energy of sGRB 170817A is also plotted at the viewing angles of the jet (cross marks). See the text for details.

with  $E_0 = 10^{52.80}$  erg,  $\theta_c = 0.059$ ,  $n = 10^{-2.51}$  cm $^{-3}$ , and  $\theta_v = 0.38 \approx 22^\circ$  (Troja et al. 2018b). Note that although we do not know whether the structure reflects that of the jet energy or of the radiative efficiency, it does not matter to the following discussions. Note also that although the jet structure could be modified after the prompt emission, namely during the propagation in the interstellar medium, it does not change the above conclusion that the jet structure is exponentially faint outward.

### 3 FORMULATION OF OFF-AXIS EMISSION

To calculate the off-axis emission from a structured jet, we generalize the formulation in Ioka & Nakamura (2001) in this section. We consider an axisymmetric jet for simplicity. Assuming that the distance to the source  $d$  is much larger than the source size, the observed flux  $F_\nu$  at a frequency  $\nu$  is obtained from volume integration of the emission coefficient  $j_\nu$  as

$$F_\nu \approx \frac{1}{d^2} \int r^2 dr \sin \theta d\theta d\phi j_\nu, \quad (2)$$

where the jet has an origin at  $r = 0$  and an axis at  $\theta = 0$  in the spherical coordinate  $(r, \theta, \phi)$ . The jet axis has a viewing angle  $\theta_v$  from the line-of-sight between the observer and the origin.

The Lorentz transformation of the emission coefficient and frequency from the lab frame (i.e., source center frame)  $j_\nu$  to the comoving frame  $j'_\nu$  is

$$j_\nu = \frac{j'_\nu}{\Gamma^2(1 - \beta \cos \theta_\Delta)^2}, \quad (3)$$

$$\nu = \frac{\nu'}{\Gamma(1 - \beta \cos \theta_\Delta)}, \quad (4)$$

respectively where we assume that the jet moves in the radial direction and thereby the angle  $\theta_\Delta$  between the jet motion

and the line-of-sight direction is given by that between the  $(\theta, \phi)$  direction and the line-of-sight direction as

$$\cos \theta_\Delta = \sin \theta \cos \phi \sin \theta_v + \cos \theta \cos \theta_v. \quad (5)$$

A single pulse of sGRBs is well approximated by instantaneous thin-shell emission at time  $t_0(\theta)$  and radius  $r_0(\theta)$ ,

$$j'_\nu = \frac{1}{(4\pi)^2 r^2} E'_\gamma(\theta) f(\nu', \theta) \delta[r - r_0(\theta)] \delta[t - t_0(\theta)], \quad (6)$$

where the angular structure of the jet is characterized by the comoving radiation energy  $E'_\gamma(\theta)$  [erg]. This is related with the radiation energy  $E_\gamma(\theta)$  and total energy  $E(\theta)$  in the lab frame as

$$\epsilon_\gamma E(\theta) = E_\gamma(\theta) = \Gamma E'_\gamma(\theta), \quad (7)$$

where the Lorentz factor  $\Gamma$  and the radiative efficiency  $\epsilon_\gamma$  also have angular structures in general. We adopt the spectral shape similar to the so-called Band function

$$f(\nu', \theta) = \frac{C}{\nu'_0(\theta)} \left( \frac{\nu'}{\nu'_0(\theta)} \right)^{1+\alpha_B} \left[ 1 + \left( \frac{\nu'}{\nu'_0(\theta)} \right)^2 \right]^{\frac{\beta_B - \alpha_B}{2}}, \quad (8)$$

with  $\alpha_B \sim -1$  and  $\beta_B \sim -2.5$  (Kaneko et al. 2006). We take the constant  $C$  so that  $\int d\nu' f(\nu', \theta) = 1$ . Note that the following discussions do not depend on the exact shape of the spectrum as long as it has a peak.

The time in the lab frame  $t$  is related with the observed time  $T$  as

$$t = T + \frac{r}{c} \cos \theta_\Delta, \quad (9)$$

where the time is measured from the merger time and we neglect the cosmological effect.

The isotropic energy is obtained from Eqs. (2), (3), (6), (7) and (9) by performing the integrals of the delta functions as

$$\begin{aligned} E_{\gamma, \text{iso}} &= \int dT \int d\nu 4\pi d^2 F_\nu \\ &= \frac{1}{4\pi} \int \sin \theta d\theta d\phi \frac{E_\gamma(\theta)}{\Gamma^4(1 - \beta \cos \theta_\Delta)^3}, \end{aligned} \quad (10)$$

where the arbitrary functions  $r_0(\theta)$  and  $t_0(\theta)$  are integrated out. We can further perform the  $\phi$  integral,

$$E_{\gamma, \text{iso}} = \int \frac{\sin \theta d\theta}{2} E_\gamma(\theta) \cdot \mathcal{B}(\theta), \quad (11)$$

where we call the last part as the beaming term,

$$\begin{aligned} \mathcal{B}(\theta) &\equiv \int_{-\pi}^{\pi} \frac{d\phi}{2\pi} \frac{1}{\Gamma^4(1 - \beta \cos \theta_\Delta)^3} \\ &= \frac{1}{2\Gamma^4} \frac{2(1 - \beta \cos \theta \cos \theta_v)^2 + (\beta \sin \theta \sin \theta_v)^2}{[1 - \beta \cos(\theta_v + \theta)]^{5/2} [1 - \beta \cos(\theta_v - \theta)]^{5/2}} \end{aligned} \quad (12)$$

Note that we can explicitly show  $E_{\gamma, \text{iso}} = E_\gamma(\theta)$  if  $E_\gamma(\theta)$  and  $\Gamma(\theta)$  are isotropic (where we can always put  $\theta_v = 0$  by changing a coordinate in the integration).

The surface brightness (i.e., the isotropic energy per solid angle) is given by

$$\frac{dE_{\gamma, \text{iso}}}{d\Omega} = \frac{1}{4\pi} \frac{E_\gamma(\theta)}{\Gamma^4(1 - \beta \cos \theta_\Delta)^3}. \quad (13)$$

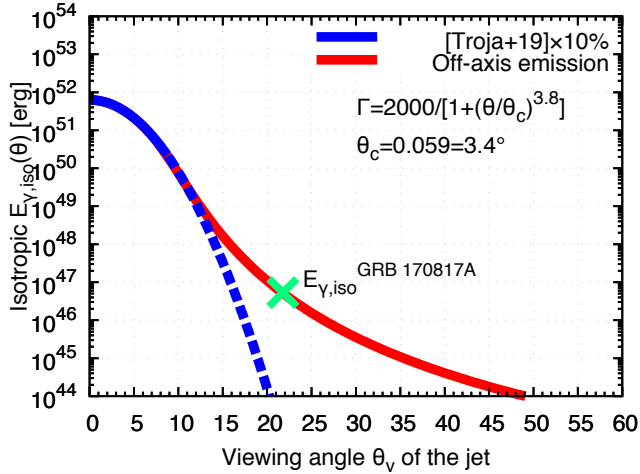


**Figure 2.** The isotropic gamma-ray energy of the off-axis emission (red line) from a structured jet in Eq. (1) (blue line) is plotted as a function of the viewing angle  $\theta_v$  of the jet. The isotropic gamma-ray energy at the viewing angle of sGRB 170817A is also plotted (green cross). We adopt the Lorentz factor profile in Eq. (16). The off-axis emission always dominates the line-of-sight emission in the outer region.

The spectral peak energy  $\nu_{\text{peak}}$  corresponds to the energy at which  $\nu dE_{\gamma,\text{iso}}/d\nu$  takes a maximum value. We can show

$$\frac{dE_{\gamma,\text{iso}}}{d\nu} = \frac{1}{4\pi} \int \sin\theta d\theta d\phi \frac{E_{\gamma}(\theta) f(\nu, \theta, \phi)}{\Gamma^4(1 - \beta \cos\theta_{\Delta})^3}, \quad (14)$$

where

$$f(\nu, \theta, \phi) = \frac{C}{\nu_0(\theta, \phi)} \left( \frac{\nu}{\nu_0(\theta, \phi)} \right)^{1+\alpha_B} \left[ 1 + \left( \frac{\nu}{\nu_0(\theta, \phi)} \right)^2 \right]^{\frac{\beta_B - \alpha_B}{2}}, \quad (15)$$

and  $\nu_0(\theta, \phi) = \nu'_0(\theta)/\Gamma(1 - \beta \cos\theta_{\Delta})$ .

## 4 OFF-AXIS EMISSION COMES FROM OFF-CENTER

### 4.1 Dominance of off-axis emission

In Fig. 2, we calculate the off-axis emission (red line) from a structured jet in Eq. (1) (blue line) with Eqs. (11) and (12). For the calculation we need the Lorentz factor, which is not well constrained from observations. As a fiducial Lorentz factor, we adopt a profile decreasing outward

$$\Gamma = \frac{\Gamma_{\text{max}}}{1 + (\theta/\theta_c)^{\lambda}}. \quad (16)$$

We take  $\Gamma_{\text{max}} = 2000$  since lower limits  $\Gamma \gtrsim 1000$  are obtained for some sGRBs like sGRB 090510 detected by *Fermi*/LAT. The index  $\lambda$  is used to match the isotropic energy with that of sGRB 170817A, and is found to be  $\lambda \approx 3.8$  for our fiducial case in Eq. (1). It is always possible to match the observed value. Note that  $\Gamma > 1$  for our range of interest. Even if the Lorentz factor profile is different, the following discussions are similar as long as it is smooth enough.

As shown in Fig. 2, the off-axis emission (red line) always dominates the line-of-sight emission (blue line) in the outer region. This is general irrespective of the uncertainty

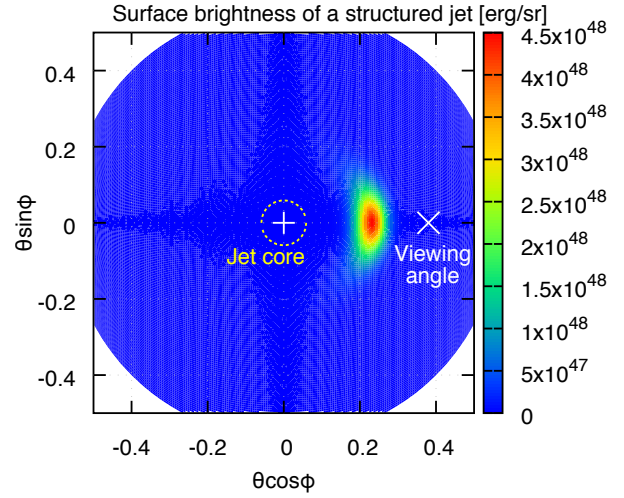


**Figure 3.** The surface brightness distribution of the jet emission is plotted on the  $(\theta \cos\phi, \theta \sin\phi)$  plane. The model parameters are the same as in Fig. 2. Most emission comes from the off-center jet, neither the jet core nor the line-of-sight jet but the middle.

of the jet structure for GW170817 because the jet energy should decrease exponentially outward in order to satisfy both the afterglow observation (i.e., the large energy at  $\theta = 0$ ) and the prompt sGRB observation (i.e., the small energy at  $\theta = \theta_v$ ) while the off-axis emission has a power-law profile  $\propto (\theta_v - \theta_c)^{-4}$  (Ioka & Nakamura 2018). Therefore if sGRB 170817A arises from a jet, it is most likely off-axis emission, not the line-of-sight emission.

### 4.2 Off-center emission

Which part of the jet makes a major contribution to the observed off-axis emission? In Fig. 3, we plot the surface brightness distribution in Eq. (13) with the same model parameters as in Fig. 2. It is remarkable that most emission comes from the off-center jet, neither the jet core nor the line-of-sight jet but the middle.

The off-center emission is also a general property of the off-axis emission irrespective of the uncertainty of the adopted jet structure for GW170817. As we can see from Eq. (11), the observed isotropic energy is determined by the product of the jet structure  $E_{\gamma}(\theta)$  and the beaming term  $\mathcal{B}(\theta)$ . These two functions are plotted in Fig. 4 (lower panel). The jet energy (green line) should decrease exponentially outward to satisfy both the observations of the afterglow and sGRB 170817A. On the other hand the beaming term (blue line) increases outward within  $\theta \lesssim \theta_v - \Gamma^{-1}$  because the beaming cone approaches the line-of-sight. The product of the decreasing function ( $E_{\gamma}(\theta)$ ) and the increasing function ( $\mathcal{B}(\theta)$ ) makes a peak in the middle, neither the jet core nor the line-of-sight.<sup>2</sup>

<sup>2</sup> This is analogous to a Gamov peak.



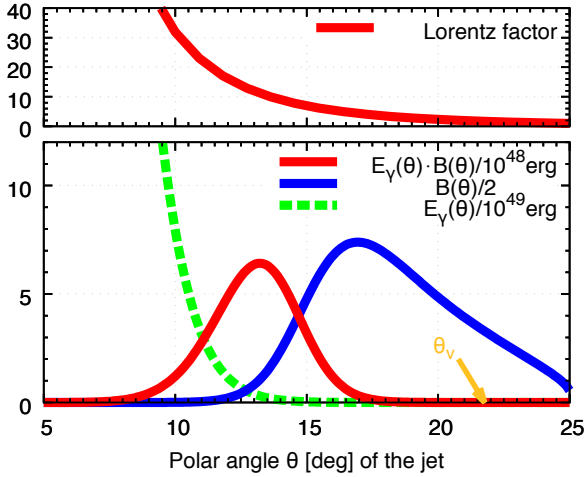


**Figure 4.** (Lower panel): The jet energy ( $E_\gamma(\theta)$ ; green line), the beaming term in Eq. (12) ( $\mathcal{B}(\theta)$ ; blue line) and their product (red line), which determines the isotropic energy in Eq. (10), are plotted as a function of the polar angle  $\theta$  of the jet. The model parameters are the same as in Fig. 2. The product of the decreasing  $E_\gamma(\theta)$  and the increasing  $\mathcal{B}(\theta)$  makes a peak in the off-center region, neither the jet core ( $\theta_c = 0.059 = 3.4^\circ$ ) nor the line-of-sight jet ( $\theta_v = 0.38$ ; orange arrow). (Upper panel): The Lorentz factor distribution in Eq. (16) is plotted as a function of  $\theta$ .

### 4.3 Compactness problem

The off-center emission is important to avoid the compactness problem. The isotropic energy of the emitting region is  $\sim 10^{48}$ – $10^{49}$  erg much smaller than that of the jet core  $\sim 10^{52}$  erg. The angular separation between the emitting region and the line-of-sight is also  $\sim 5^\circ$ – $10^\circ$  much smaller than the top-hat case  $\theta_v - \theta_c \sim 20^\circ$ . Taking into account that the Lorentz factor at the emitting region  $\Gamma \sim 10$  (see upper panel in Fig. 4) is smaller than that of the jet core  $\Gamma \sim 10^3$ , we can show that the compactness problem is not crucial (Matsumoto et al. 2019).<sup>3</sup>

### 4.4 Spectral Amati relation

The off-center emission could also solve the seemingly inconsistency with the Amati relation between the spectral peak energy and the isotropic energy. Actually the off-center emission does not satisfy the Amati relation as argued previously. However the jet core can satisfy the Amati relation. The point is that the off-center jet is different from the jet core. The classical sGRBs are emitted by the on-axis jet core and hence satisfy the Amati relation, where the off-center region is too faint to observe. The off-center region is observable only for an off-axis event like sGRB 170817A, in which the core emission is severely de-beamed and suppressed. Usually an off-axis event is difficult to find because they are faint. The jet structure is exponentially faint outward and is more or less top-hat-like. Thus it is easy to understand that the off-axis event is difficult to find without any other signature like GWs.

<sup>3</sup> The innermost part of the emitting region could suffer from the compactness problem.

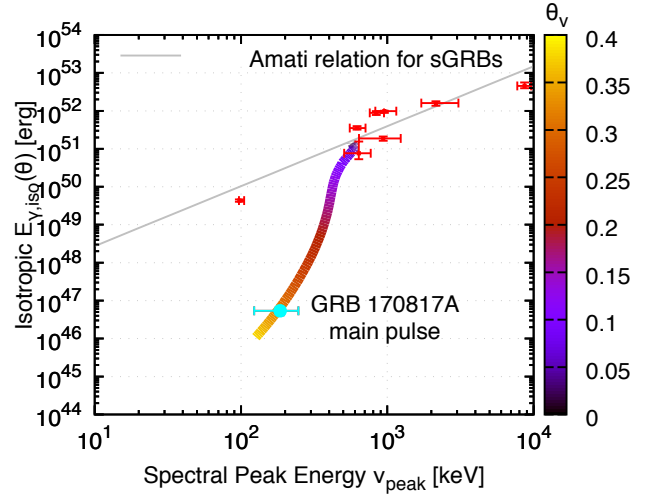


**Figure 5.** An example where the on-axis emission from the jet core satisfies the Amati relation and the off-axis emission from the off-center jet reproduces sGRB 170817A is constructed on the plane of the spectral peak energy  $\nu_{\text{peak}}$  and isotropic energy  $E_{\gamma,\text{iso}}$ . The color of the line shows the viewing angle of the jet  $\theta_v$ . The model is compared with the observations of sGRBs, which satisfies the Amati relation (grey solid line). Note that Amati relation for sGRBs is  $\sim 100$  times dimmer than that for long GRBs at the same peak energy  $\nu_{\text{peak}}$ , which is determined by the sGRBs used in Tsutsui et al. (2013) (red filled squares).

In Fig. 5, we construct a concrete example of the off-axis emission where the on-axis emission from the jet core satisfies the Amati relation and the off-axis emission from the off-center jet reproduces sGRB 170817A. We adjust the comoving spectral energy  $\nu'_0(\theta)$  in Eq. (8) as  $\nu'_0(\theta) = 0.15 \text{ keV} [1 + (\theta/\theta_c)^{3.4}]$  by changing the power-law index (3.4 here) with the same model parameters as in Figs. 2–4. Note that the product with Eq. (16)  $\Gamma(\theta)\nu'_0(\theta)$  (i.e., lab-frame spectral energy) is a slowly decreasing function of  $\theta$ . The Amati relation is satisfied as long as the viewing angle is about the core size  $\theta_v \sim \theta_c$ , where  $\theta_c = 0.059 = 3.4^\circ$  for our fiducial case. As the viewing angle becomes large, the spectral relation deviates from the Amati relation and approaches the point of sGRB 170817A. If this interpretation is correct, future observations will find outliers of Amati relation, although the event rate of the outliers is very small because the jet structure is exponentially faint outward.

## 5 SUMMARY AND DISCUSSIONS

In this paper we identify the spectral puzzle and propose a natural solution in the off-axis jet model for sGRB 170817A associated with GW170817. Taking both the afterglow and prompt sGRB 170817A into account, we first clarify that the jet structure should be exponentially faint outward, so that the off-axis emission dominates the line-of-sight emission at a large viewing angle. Given that, we generally show that the off-axis emission comes from an off-center jet, neither the jet core nor the line-of-sight but the middle. Because the off-center jet is much less energetic and much closer to the line-of-sight than the jet core, the compactness problem is avoidable. In addition, the Amati relation may be violated

as in sGRB 170817A because the off-center jet is different from the jet core that satisfies the Amati relation.

The off-center jet is too faint to find for ordinary observations without any other messengers like GWs, high-energy gamma-rays (Murase et al. 2018) and neutrinos (Kimura et al. 2018). Even if it is detected in gamma-rays, the redshift is not determined without follow-up observations. Since the jet structure is exponentially faint outward and hence top-hat-like, the event rate of detecting the off-center jet is very small. This explains why there are not so much outliers to the Amati relation. Conversely the off-axis model predicts outliers to the Amati relation once many events are observed. It is reported that there are similar bursts with similar spectrum to sGRB 170817A among previous sGRBs (Burns et al. 2018; Troja et al. 2018c; von Kienlin et al. 2019). They could be off-axis events like sGRB 170817A.

The off-axis model predicts brighter events at smaller viewing angles than sGRB 170817A. Taking the inclination dependence of the GW amplitude into account, the probability of observing the viewing angle  $\theta_v \lesssim 20^\circ$ ,  $15^\circ$  and  $10^\circ$  is  $\sim 20\%$ ,  $10\%$  and  $5\%$ , respectively (Lamb & Kobayashi 2017). Therefore future multi-messenger observations, in particular with GWs and gamma-rays, can test the off-axis jet model in GW170817. However, the exact event rate of the off-axis event depends on the outer structure of the jet, which is not constrained by the afterglow observations of GW170817 (see *dashed lines* in Figs. 1 and 2). It is necessary to observe earlier afterglows than  $\sim 10$  days to probe the off-center jet that is relevant to the off-axis emission. In addition the viewing angle of GW170817 still has an uncertainty  $\theta_v \sim 14^\circ\text{--}28^\circ$  even after the VLBI observations of superluminal motion because it depends on the jet core size and the sideways expansion during the propagation in the interstellar medium, which also depends on the unobserved off-center structure. It is a future problem to encompass the uncertainty of the event rate.

It is not known how the jet structure is formed in particular in the off-center region for sGRB 170817A. There are several possibilities. First the jet itself could have a structure. Even if the jet has a weak outer structure, it is cut off during the jet propagation through the merger ejecta. However the baryon load could be angular dependent, leading to a different angular expansion and hence a jet structure after the jet breakout from the merger ejecta. Note that baryon may be loaded at the base of the jet launch as well as during the jet propagation. Second the off-center region could be a cocoon, which is produced by the shocked jet and shocked ejecta during the jet propagation. Although a typical velocity of the cocoon is sub-relativistic, an imperfect mixing between the shocked jet and shocked ejecta make a high-entropy cocoon surrounding a jet, which could lead to a jet structure. We did not also consider several effects such as the temporal evolution, the photosphere, the high-energy spectral cutoff and so on. These are interesting future problems.

## ACKNOWLEDGEMENTS

The authors would like to thank J. Granot, H. Hamidani, K. Hotokezaka, K. Kashiyama, T. Kinugawa, S. Kisaka, K. Kyutoku, G. P. Lamb, A. Levinson, T. Matsumoto, T. Piran,

G. Ryan, M. Shibata, K. Takahashi and R. Yamazaki for useful discussions. This work is partly supported by JSPS KAKENHI nos. 18H01215, 17H06357, 17H06362, 17H06131, 26287051 (KI) and 15H02087 (TN).

## REFERENCES

- Abbott B. P., et al., 2017a, *Physical Review Letters*, **119**, 161101  
 Abbott B. P., et al., 2017b, *ApJ*, **848**, L12  
 Abbott B. P., et al., 2017c, *ApJ*, **848**, L13  
 Alexander K. D., et al., 2017, *ApJ*, **848**, L21  
 Amati L., et al., 2002, *A&A*, **390**, 81  
 Berger E., 2014, *ARA&A*, **52**, 43  
 Burns E., et al., 2018, *ApJ*, **863**, L34  
 D’Avanzo P., et al., 2018, *A&A*, **613**, L1  
 Eichler D., Livio M., Piran T., Schramm D. N., 1989, *Nature*, **340**, 126  
 Fong W., Berger E., Margutti R., Zauderer B. A., 2015, *ApJ*, **815**, 102  
 Ghirlanda G., et al., 2018, arXiv e-prints,  
 Goldstein A., et al., 2017, *ApJ*, **848**, L14  
 Goodman J., 1986, *ApJ*, **308**, L47  
 Gottlieb O., Nakar E., Piran T., Hotokezaka K., 2018, *MNRAS*, **479**, 588  
 Granot J., Guetta D., Gill R., 2017, *ApJ*, **850**, L24  
 Granot J., Gill R., Guetta D., De Colle F., 2018, *MNRAS*, **481**, 1597  
 Haggard D., Nynka M., Ruan J. J., Kalogera V., Cenko S. B., Evans P., Kennea J. A., 2017, *ApJ*, **848**, L25  
 Hallinan G., et al., 2017, arXiv:1710.05435,  
 Ioka K., Nakamura T., 2001, *ApJ*, **554**, L163  
 Ioka K., Nakamura T., 2018, *Progress of Theoretical and Experimental Physics*, **2018**, 043E02  
 Ioka K., Levinson A., Nakar E., 2019, *MNRAS*, **484**, 3502  
 Kaneko Y., Preece R. D., Briggs M. S., Paciesas W. S., Meegan C. A., Band D. L., 2006, *ApJS*, **166**, 298  
 Kasliwal M. M., et al., 2017, arXiv:1710.05436,  
 Kimura S. S., Murase K., Bartos I., Ioka K., Heng I. S., Mészáros P., 2018, *Phys. Rev. D*, **98**, 043020  
 Kisaka S., Ioka K., Nakamura T., 2015, *ApJ*, **809**, L8  
 Kisaka S., Ioka K., Sakamoto T., 2017, *ApJ*, **846**, 142  
 Kisaka S., Ioka K., Kashiyama K., Nakamura T., 2018, *ApJ*, **867**, 39  
 Kumar P., Granot J., 2003, *ApJ*, **591**, 1075  
 Lamb G. P., Kobayashi S., 2017, *MNRAS*, **472**, 4953  
 Lamb G. P., Kobayashi S., 2018, *MNRAS*, **478**, 733  
 Lamb G. P., et al., 2019, *ApJ*, **870**, L15  
 Lazzati D., Perna R., Morsony B. J., Lopez-Camara D., Cantiello M., Ciolfi R., Giacomazzo B., Workman J. C., 2018, *Physical Review Letters*, **120**, 241103  
 Lyman J. D., et al., 2018, *Nature Astronomy*, **2**, 751  
 Margutti R., et al., 2017, *ApJ*, **848**, L20  
 Margutti R., et al., 2018, *ApJ*, **856**, L18  
 Matsumoto T., Nakar E., Piran T., 2019, *MNRAS*, **483**, 1247  
 Mészáros P., Rees M. J., Wijers R. A. M. J., 1998, *ApJ*, **499**, 301  
 Mooley K. P., et al., 2018a, *Nature*, **554**, 207  
 Mooley K. P., et al., 2018b, *Nature*, **561**, 355  
 Mooley K. P., et al., 2018c, *ApJ*, **868**, L11  
 Murase K., et al., 2018, *ApJ*, **854**, 60  
 Murguia-Berthier A., Montes G., Ramirez-Ruiz E., De Colle F., Lee W. H., 2014, *ApJ*, **788**, L8  
 Nagakura H., Hotokezaka K., Sekiguchi Y., Shibata M., Ioka K., 2014, *ApJ*, **784**, L28  
 Nakar E., 2007, *Phys. Rep.*, **442**, 166  
 Nakar E., Gottlieb O., Piran T., Kasliwal M. M., Hallinan G., 2018, *ApJ*, **867**, 18

- Paczynski B., 1986, [ApJ](#), **308**, L43
- Ruan J. J., Nynka M., Haggard D., Kalogera V., Evans P., 2018, [ApJ](#), **853**, L4
- Savchenko V., et al., 2017, [ApJ](#), **848**, L15
- Troja E., et al., 2017, [arXiv:1710.05433](#),
- Troja E., et al., 2018a, [MNRAS](#), p. L60
- Troja E., et al., 2018b, [arXiv e-prints](#), p. [arXiv:1808.06617](#)
- Troja E., et al., 2018c, [Nature Communications](#), **9**, 4089
- Tsutsui R., Yonetoku D., Nakamura T., Takahashi K., Morihara Y., 2013, [MNRAS](#), **431**, 1398
- Veres P., et al., 2018, [arXiv e-prints](#), p. [arXiv:1802.07328](#)
- Yamazaki R., Ioka K., Nakamura T., 2002, [ApJ](#), **571**, L31
- Yamazaki R., Ioka K., Nakamura T., 2018, [Progress of Theoretical and Experimental Physics](#), **2018**, 033E01
- Yonetoku D., Murakami T., Nakamura T., Yamazaki R., Inoue A. K., Ioka K., 2004, [ApJ](#), **609**, 935
- Zhang B., Mészáros P., 2002, [ApJ](#), **571**, 876
- van Eerten H., Zhang W., MacFadyen A., 2010, [ApJ](#), **722**, 235
- von Kienlin A., et al., 2019, [arXiv e-prints](#), p. [arXiv:1901.06158](#)

This paper has been typeset from a  $\text{\TeX}/\text{\LaTeX}$  file prepared by the author.